



**HAL**  
open science

**Effects of solar radiations on stratum corneum hydration: Part I, protective role of skin surface lipids**  
Ali Assi, Rime Michael-Jubeli, H el ene Duplan, Arlette Baillet-Guffroy, Carine Jacques-Jamin, Ali Tfayli

► **To cite this version:**

Ali Assi, Rime Michael-Jubeli, H el ene Duplan, Arlette Baillet-Guffroy, Carine Jacques-Jamin, et al..  
Effects of solar radiations on stratum corneum hydration: Part I, protective role of skin surface lipids.  
Journal of Biophotonics, 2023, 16 (8), 10.1002/jbio.202300055 . hal-04521976

**HAL Id: hal-04521976**

**<https://hal.science/hal-04521976>**

Submitted on 26 Mar 2024

**HAL** is a multi-disciplinary open access archive for the deposit and dissemination of scientific research documents, whether they are published or not. The documents may come from teaching and research institutions in France or abroad, or from public or private research centers.

L'archive ouverte pluridisciplinaire **HAL**, est destin ee au d ep ot et  a la diffusion de documents scientifiques de niveau recherche, publi es ou non,  emanant des  tablissements d'enseignement et de recherche fran ais ou  trangers, des laboratoires publics ou priv es.

## RESEARCH ARTICLE

# Effects of solar radiations on stratum corneum hydration: Part I, protective role of skin surface lipids

Ali Assi<sup>1</sup>  | Rime Michael-Jubeli<sup>1</sup> | H el ene Duplan<sup>2</sup> |  
Arlette Baillet-Guffroy<sup>1</sup> | Carine Jacques-Jamin<sup>2</sup> | Ali Tfayli<sup>1</sup> 

<sup>1</sup>Lip(Sys)<sup>2</sup>, Chimie Analytique Pharmaceutique (EA4041 Groupe de Chimie Analytique de Paris-Saclay), Universit  Paris-Sud, Universit  Paris-Saclay, Orsay, France

<sup>2</sup>Pierre Fabre Dermo-cosm tique, Centre R&D Pierre Fabre, Toulouse, France

## Correspondence

Ali Tfayli, Lip(Sys), Chimie Analytique Pharmaceutique (EA4041 Groupe de Chimie Analytique de Paris-Saclay), Universit  Paris-Sud, Universit  Paris-Saclay, Orsay F-91400, France.  
Email: [ali.tfayli@universite-paris-saclay.fr](mailto:ali.tfayli@universite-paris-saclay.fr)

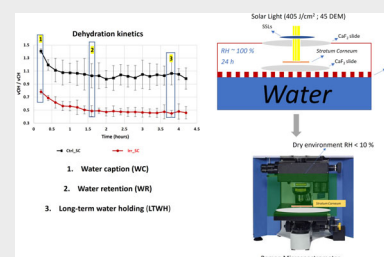
## Abstract

This study used Raman spectroscopy to develop a new approach to evaluate the effects of solar radiation on the stratum corneum (SC). The method measures the SC's hydration and dehydration kinetics by calculating the  $\nu\text{OH}/\nu\text{CH}$  ratio to monitor the relative water content during the drying process.

The study also investigated the role of skin surface lipids (SSLs) in protecting the SC from solar radiation. The SSLs film is a complex mixture of free fatty acids, triglycerides, wax esters, squalene, free and esterified cholesterols, that play a crucial role in the skin's barrier function. The results showed that solar radiation alters the water content and balance within the SC, and SSLs provide protection by acting as an optical filter by absorbing some of the energy of the solar light. This is confirmed by high temperature gas chromatography coupled to mass spectrometry analyses by revealing a decrease in specific lipids after irradiating the SSLs.

## KEYWORDS

HT-GC/MS, hydration, skin surface lipids, solar radiations, stratum corneum



## 1 | INTRODUCTION

The upper layer of the skin, the stratum corneum (SC) represents the main barrier against external chemical and biological aggressions and regulates water loss [1–5]. It is the body's first line of defense against environmental stresses such as solar radiations. The SC is composed of three major components: corneocytes, corneodesmosomes, and an intercellular lipid matrix [4] which is responsible for the formation and maintenance of the skin barrier [6–8].

SC hydration has been widely studied to understand the phenomena influencing skin dryness disorders usually found in dermatology and in cosmetic applications [9]. It is well-established that water plays an important role for maintaining a normal functioning of the skin and especially the SC [10]. In return, the latter is responsible for controlling the skin hydration by three different mechanisms: barrier function, water binding, and water diffusion within the SC [9]. The organization and the lateral packing of SC lipids are essential to maintain the

This is an open access article under the terms of the [Creative Commons Attribution-NonCommercial-NoDerivs](https://creativecommons.org/licenses/by-nc-nd/4.0/) License, which permits use and distribution in any medium, provided the original work is properly cited, the use is non-commercial and no modifications or adaptations are made.

  2023 The Authors. *Journal of Biophotonics* published by Wiley-VCH GmbH.

barrier function properties. A pure liquid crystal system or a solid system of SC lipids induces rapid water loss through the bilayer. Thus, to prevent water loss and to maintain an optimal barrier function, it is necessary to maintain the balance between these two phases [11, 12]. In addition, the presence of natural moisturizing factors (NMFs) which are hygroscopic molecules helps water absorption and binding [9].

A balance between these mechanisms maintains equilibrated SC hydration. However, changes in this balance may lead to a dermatologic condition known as “dry skin” which may give rise to various infections, allergies, and eczemas [13].

Although they can have beneficial effects such as by stimulating the production of vitamin D [14], solar irradiation effect on human health depends on the amount and type of radiations that reaches the body [15]. They can result in the formation of free radicals and contribute in the deterioration of epidermal and dermal structures inducing photoaging or, in extreme cases, skin cancer [16].

On the SC, UV solar radiations are among the external insults that alter the skin barrier. In vivo studies showed their impact on the decrease of carotenoids [1, 17–21] and the isomerization of the urocanic acid (UCA) from its *trans* form to its *cis* form Refs. [22, 23]. Other studies highlighted the thickening of the SC [24]. Finally, the increase of the transepidermal water loss was commonly highlighted [25–29], indicating an altered barrier against water loss and thus a deterioration in the water homeostasis and water holding capacities may be suggested.

Contrary to in vivo observations, the effect of UV irradiations on the barrier function of excised SC sheets is only observable when using very high doses. Biniek et al. [30] applied  $\sim 160 \text{ J/cm}^2$  of  $\text{UV}_B$  and showed a decrease in the  $\text{CH}_2$  symmetric and asymmetric stretching on the infrared spectra of the irradiated samples indicating a decrease in the barrier function. The applied doses are over 5000 times higher than minimal erythema dose (MED). It is thus important to highlight the effect of regularly used UV doses on SC.

In the current study, we first proposed a new approach to evaluate the effect of solar radiations on the SC. It is based on the SC water homeostasis, in particular the water caption (WC) and dehydration kinetics. Ex vivo measurements were performed on isolated SC using Raman microspectroscopy. The global water content was evaluated using the area under the curve (AUC) of the OH stretching band ( $3100\text{--}3700 \text{ cm}^{-1}$ ). The  $\nu\text{OH}/\nu\text{CH}$  ratio was calculated in order to follow-up the drying process and to monitor the relative water content in the whole SC. The AUC of CH stretching band was measured in the range of  $2800\text{--}3000 \text{ cm}^{-1}$  [31–33].

Even though the barrier property of skin is localized in the SC, the hydrolipidic film participates to this barrier function [12, 34–37]. It is composed of sweat and skin surface lipids (SSLs). SSLs are composed of a complex of lipids that come either from sebaceous secretion such as triglycerides, wax esters, and squalene, from desquamation such as free and esterified cholesterols, or from both, like free fatty acids (FFAs) [38–41]. In addition, triglycerides are partially hydrolyzed, producing FFAs, diglycerides, monoglycerides, and glycerol under the effect of lipase-producing microorganisms of human skin flora [42–44]. Moreover, antioxidants like vitamin E can be found within the hydrolipidic film [35, 45–47].

In a second time, we explored the role of SSLs in the protection of water homeostasis in the SC against solar radiations. SSLs films were added directly at the surface of the SC before irradiation or deposited on a  $\text{CaF}_2$  slide. For the latter, the irradiation was performed through the SSLs layer on the slide.

Finally, to understand the effect of solar radiations on SSLs, high temperature gas chromatography–mass spectrometry (HTGC–MS) analyses were performed on control and irradiated SSLs with different doses. HT-GC/MS is a widely used method for analyzing complex mixtures and is well-adapted for a comprehensive study of SSLs [47, 48].

## 2 | MATERIALS AND METHODS

### 2.1 | SC samples preparation

The SC layers were prepared from human abdominal skin using a method described previously [9]. Three SC samples from three different donors were used for each experiment condition. Three repetitions per condition were performed to monitor the water desorption (WD) kinetics of hydrated SC.

To study the impact of UV solar radiations on the hydration properties of the SC and to evaluate the protective role of SSLs against these radiations, five experimental conditions were prepared as follows (Table 1):

### 2.2 | SSLs preparation

SSLs were provided from the Center of Research Pierre Fabre Dermo Cosmetics (PFDC, Toulouse, France) and obtained from the forehead zone of healthy volunteers.

For Raman measurements,  $250 \mu\text{L}$  of SSLs were diluted in physiological serum to obtain a concentration of  $2 \text{ mg/mL}$ . For SC coated with SSLs experiments,  $2.5 \mu\text{L}$  were spread on the surface of the SC.

For HTGC/MS analyses,  $250 \mu\text{L}$  of this solution was prepared in chloroform. SSLs were derivatized in prior by

trimethylsilylation. This reagent consisted of BSTFA/pyridine, 50:50 (v/v). SSLs were trimethylsilylated at room temperature for 30 min with 200  $\mu\text{L}$  of reagent. The excess reagent was then removed under nitrogen flow, and the dried residue was dissolved in 250  $\mu\text{L}$  of chloroform.

### 2.3 | Solar irradiation of SC and SSLs

SC samples and SSLs were irradiated using a solar simulator 16S-300 from solar light company which produces a spectrum close to the solar spectrum. The power used for the irradiation was 0.45  $\text{W}/\text{cm}^2$ . This power was measured using a pyranometer (Glenside, USA).

To evaluate the effect of solar light on hydration kinetics, SC samples were irradiated for 15 min (Table 2).

To evaluate the impact of irradiation on SSLs composition; SSLs were irradiated at two different times (180 and 360 min).

### 2.4 | High temperature gas chromatography–mass spectrometry (HTGC–MS)

A Thermo Scientific (Austin, TX) gas chromatography unit (Trace GC Ultra) equipped with an on-column injector was coupled to a quadrupole DSQII mass spectrometer via a high-temperature interface. The separation was achieved

TABLE 1 Prepared experimental conditions.

1	SC non-coated with SSLs and non-irradiated	Ctrl-SC
2	SC non-coated with SSLs and irradiated	Irr-SC
3	SC coated with SSLs and non-irradiated	Ctrl SC + SSLs
4	SC coated with SSLs and irradiated	Irr-SC + SSLs
5	SC irradiated through SSLs placed on $\text{CaF}_2$ slide	SC-Irr-SSLs

TABLE 2 The different doses applied to skin surface lipids during irradiation in  $\text{J}/\text{cm}^2$ .

Time (min)	15	180	360
Sample	SC	SSLs	SSLs
Analyses	Raman	GC/MS	GC/MS
$E$ ( $\text{J}/\text{cm}^2$ ), total solar spectrum	405	4860	9720
$E$ ( $\text{J}/\text{cm}^2$ ), total UV radiations	8.55	102.6	205.2
$E$ ( $\text{J}/\text{cm}^2$ ), $\text{UV}_B$ radiations	1.35	16.2	32.4
$E$ ( $\text{J}/\text{cm}^2$ ), $\text{UV}_A$ radiations	7.2	86.4	172.8
Minimal erythral dose	45 MED	540 MED	1080 MED

using a 30 m  $\times$  0.32 mm ZB-5HT capillary column (Phenomenex, Torrance, CA) coated with 0.1  $\mu\text{m}$  of 5% diphenyl/95% dimethylpolysiloxane, connected to a 5 m, 0.32 mm HT-deactivated tubing guard column.

Helium was used as a carrier gas at a constant flow of 2 mL/min. The injector and transfer line temperatures were set to 60 and 350°C, respectively. The oven temperature was programmed from 60 to 240°C at 5°C/min; 240 to 320°C at 2.5°C/min; and 320 to 350°C at 1°C/min. The operating conditions for electronic impact mass spectrometry (EI–MS) were source temperature at 220°C, ionizing energy at 70 eV, and scan range from  $m/z$  45 to 1000 with a period of 1 s. EI mass spectra were recorded in the total ion current (TIC) monitoring mode (Figure 1).

### 2.5 | Raman microspectrometer

A confocal Raman microspectrometer LabRam HR Evolution (Horiba Scientific, Lille, France) was used for spectral acquisition. A video image of the sample was used for accurate positioning of the laser spot on the sample. A 633 nm He:Ne laser (Toptica Photonics, Munich, Germany), was used. A long focal 100X objective/NA = 0.9 (Olympus, Tokyo, Japan) was used to focus the laser light on the surface of the sample and to collect the back scattered light. The confocal pinhole was set to 200  $\mu\text{m}$ . The penetration depth was from  $-10$  to 30  $\mu\text{m}$  with a step size of 2  $\mu\text{m}$  repeated 21 times. The depth resolution was around 2  $\mu\text{m}$ .

The collected light was filtered through an edge filter and dispersed with a 4  $\text{cm}^{-1}$  spectral resolution using a 300  $\mu\text{m}$  slit and a holographic grating of 300 grooves/mm. The Raman Stokes signal was recorded with a Synapse Charge-Coupled Device detector: CCD camera (Andor Technology, Belfast, UK) containing 1024  $\times$  256 pixels. Spectral acquisition was performed using the LabSpec 6 software (Horiba Scientific, Lille, France). Raman measurements were performed on each depth in the 400–3800  $\text{cm}^{-1}$  spectral range. For each scan, a 5 s exposure

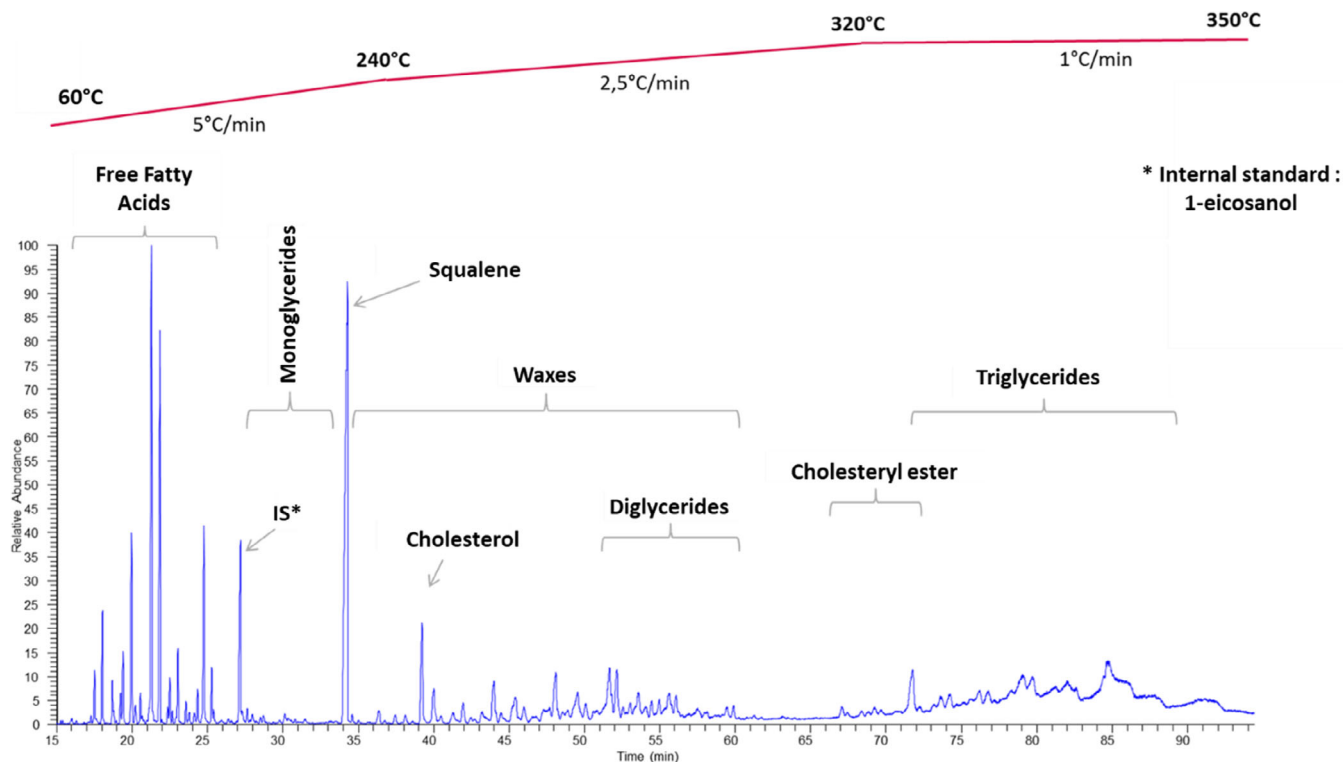


FIGURE 1 HTGC-MS profile of a trimethylsilylated SSLs sample.

time with two accumulations was used. All spectra were smoothed using Savitzky–Golay algorithm and baseline corrected using an automatic polynomial function.

## 2.6 | Raman spectroscopy of SC water loss

Raman spectroscopy was performed on SC samples equilibrated at high humidity ( $\sim 100\%$  RH) and then placed in a dry environment to study WD. A humidity-controlled chamber, based on an airflow principle, was built around the microscope. A hygrometer/thermometer (with  $\pm 2\%$  accuracy) was used to measure relative humidity. The humidity was set to 10% RH. To obtain the desired relative humidity a dry airflow was used in the chamber with a flow rate of 3 L/min [49].

The WD analysis was carried out on isolated SC settled onto  $\text{CaF}_2$  slides. As the SC is fixed on a glass slide, desorption occurs only from one side of the SC, similar to in vivo drying [31–33]. WD kinetics of hydrated SC samples in a dry environment were studied.

Raman profiles acquisitions were performed on SC from  $-10\ \mu\text{m}$  (before the SC surface) to  $30\ \mu\text{m}$  under the surface repeated 21 times (from the beginning of the drying process [t0] to 4.25 h of dehydration).

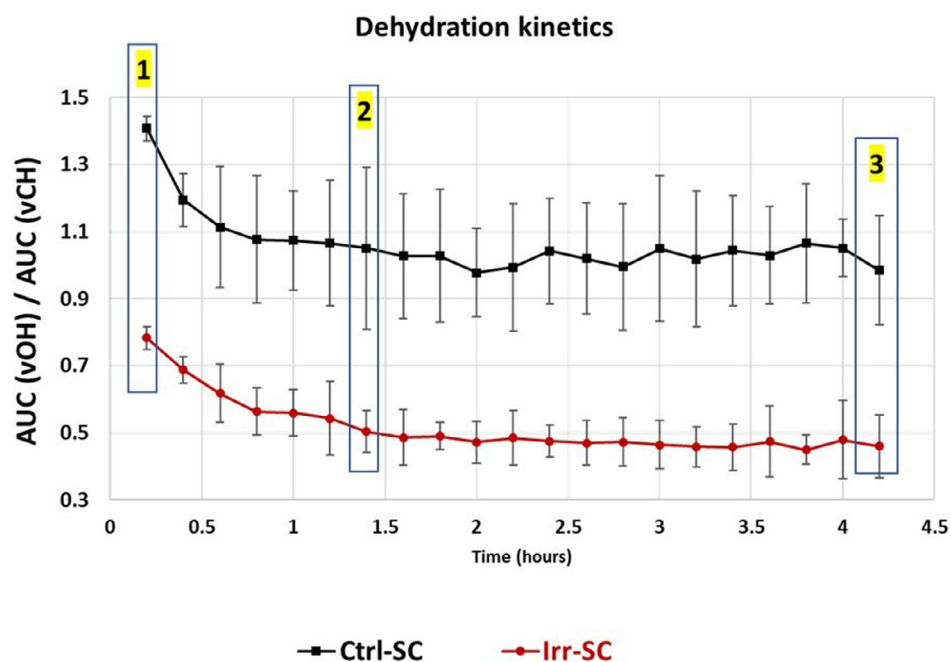
To follow-up the drying process and to monitor the relative water content in the whole SC, vOH/vCH ratio was calculated from each spectrum in the spectral profiles. The global relative content for each spectral profile was obtained from its AUC between 0 and  $12\ \mu\text{m}$  (limits of the SC). A unique value is thus obtained for each in-depth profile.

WD kinetics were repeated 3 times for each experimental condition. The final dehydration profile kinetic can be represented as the plot of the mean  $\pm$  standard error values against time (Figure 2).

## 2.7 | Statistical analyses

Analysis of variance (ANOVA) is one of the most widely used tests for experimental data. It is a powerful method to compare differences between the means of several groups. The test compares the variability of each population (intra-group variances) and that of grouped populations (inter-group variance) and thus determines whether the groups are significantly different. A pairwise comparison based on Bonferroni test was performed. For each experimental condition, the average results of the measurements on SC were presented as mean  $\pm$  standard deviation.

**FIGURE 2** Variation of the global water content in the SC during a drying process. Mean  $\pm$  standard error values of vOH/vCH ratios are plotted against time.



### 3 | RESULTS AND DISCUSSION

#### 3.1 | Characterization of dehydration kinetics

As described in Section 2, “Raman spectroscopy of SC water loss” paragraph, in order to follow the drying process and to monitor the amount of water present throughout the entire SC, the vOH/vCH ratio was determined for each spectrum in the spectral profiles. The overall relative water content for each spectral profile was then determined by calculating its AUC between 0 and 12  $\mu\text{m}$  (the limits of the SC). This allowed for a single value to be obtained for each profile at every depth.

The kinetic profile of the final dehydration can be represented by plotting the mean  $\pm$  standard error values against time (Figure 2).

The global water is represented in Y-axis by plotting the ratio between OH stretching band (water) and CH stretching band (lipids and proteins). The X-axis represents the time.

Different information can be obtained from the drying profiles, that is:

1. The *WC* capacity can be obtained after 24 h of SC stabilization at 100% relative humidity. WC can be obtained when data is registered directly after the 100% RH stabilization. This corresponds to the point at the beginning of the drying process (Figure 2/flag no. 1).
2. The *water retention (WR)* capacity represents the remaining water after 1.5 h of the beginning of the

drying process. This delay corresponds to the end of the sharp decrease in water content (Figure 2/flag no. 2).

3. The *water desorption percentage (WD%)* can be obtained by calculating the ratio:  $(WC - WR)/WC * 100$ . Low values indicate good resistance to WD while an increase is associated to an alteration in the barrier properties against water loss.
4. The *long-term water holding (LTWH)* capacity represents the water ratio observed at the end of the drying process (Figure 2/flag no. 3).
5. The *global water loss percentage (GWL%)* is obtained by calculating the ratio:  $(WC - LTWH)/WC * 100$ . Low GWL% values are correlated to good water-holding capacities.

In order to evaluate the effect of solar radiations on dehydration kinetics (Irr-SC) and the impact of adding SSLs at the surface of the SC (Ctrl SC + SSLs and Irr-SC + SSLs) or irradiation through a SSLs layer; (SC-Irr-SSLs) WC, water retention (WR), and LTWH of all drying kinetics profiles are plotted in Figure 3A for WC, Figure 3B for WR, and Figure 3C for LTWH.

Table 3 displays the WD% and the GWL%.

#### 3.2 | Solar radiations alter hydration properties of SC

After solar radiations (405 J/cm<sup>2</sup>), the hydration properties of the SC were significantly altered. WC capacity (Figure 3A) decreased of almost 44% when irradiated SC (Irr-SC) is compared to control (Ctrl-SC).

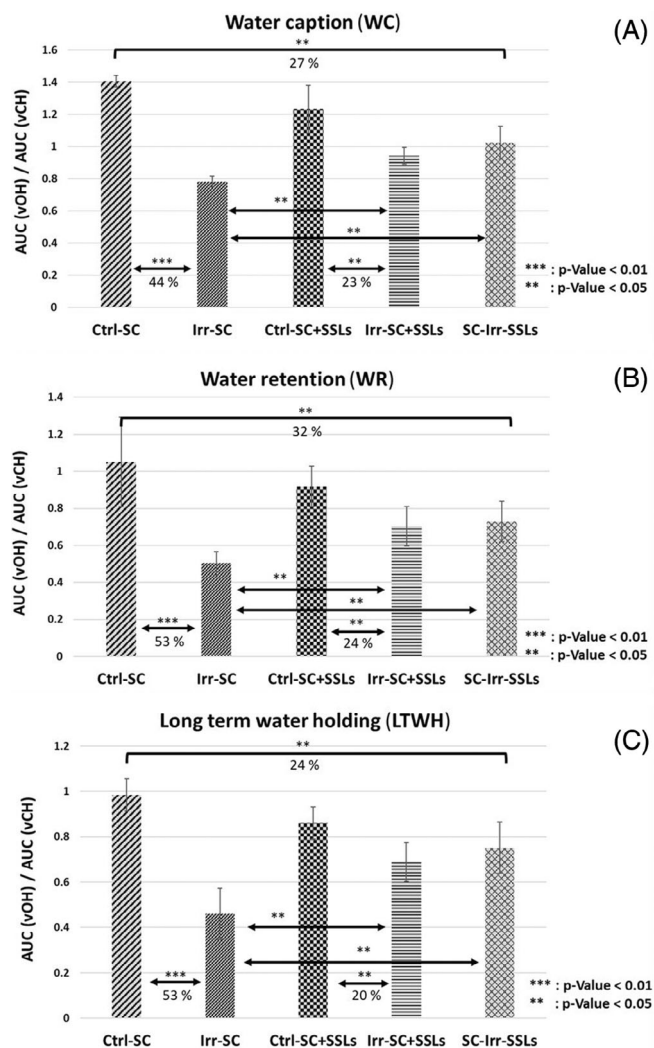


FIGURE 3 A: water caption (WC), B: water retention (WR), and C: long-term water holding (LTWH).

The same observations were obtained for WR with a decrease of almost 53% (Figure 3B) and LTWH with a 54% decrease (Figure 3C).

In addition to the information directly related to water content, relative values informed about the state of the SC barrier against water loss, that is, WD% showed a 36% loss of water content after 1.5 h for Irr-SC against only 26% for Ctrl-SC (Table 3).

GWL% observed after 4.2 h was 42% for Irr-SC and 39% for Ctrl-SC (Table 3).

These values indicate that the final relative water loss after 4.2 h of equilibration at 10%RH results in close GWL% values between control and irradiated SC. Meanwhile, a major part of the relative water loss is observed at the first part of the drying process for Irr-SC (WD%) compared to control.

It is important to note that the absolute water content remained higher for control SC all over the hydration and drying experiment.

In addition to the global water content, the tightly, partially, and un-bound water were evaluated by deconvoluting of the OH stretching (vOH) band ( $3100\text{--}3700\text{ cm}^{-1}$ ).

The spectral deconvolution of the OH stretching band showed a marked decrease in the relative amount of tightly bound water ( $p$ -value 0.01) compared to partially bound and unbound water (data not shown). This observation may be related to modifications in the molecular sites presenting Hydrogen bonding possibilities, for example, proteins and polar heads of lipids. Furthermore, to assess the impact of solar light on protein conformations, we were interested in the Amid I region ( $1600\text{--}1700\text{ cm}^{-1}$ ). The analyses of Raman features related to proteins secondary structures showed a nonsignificant increase in the ratio between random coils on one hand and alpha helices and beta sheets on the other hand. In the end, conformations of SC lipids were evaluated by comparing the peaks at  $1060$  and  $1130\text{ cm}^{-1}$  (vC-C of *trans* conformations) associated with the ordered state and the peak at  $1080\text{ cm}^{-1}$  (vC-C of *gauche* conformations). The lateral packing of SC lipids was also studied using the CH stretching bands in the range of  $2800\text{--}3000\text{ cm}^{-1}$ . No significant modifications were observed in the spectral descriptors of the SC lipids conformational order and lateral packing, (Data not shown).

In their work on the effect of UV<sub>B</sub> radiations on the barrier function and the mechanical integrity of the SC, Biniek et al. [30] applied  $\sim 160\text{ J/cm}^2$  of UV<sub>B</sub> and showed a decrease in the CH<sub>2</sub> symmetric and asymmetric stretching on the infrared spectra of the irradiated samples indicating a decrease in the barrier function. The applied doses are  $\sim 118$  times higher compared to the doses applied in the current study.

Even though the applied dose in our study does not induce detectable changes in the Raman spectra, its impact on the alteration of the WC and the dehydration kinetics is clearly observed. These observations are in concordance with different *in vivo* clinical evaluation showing an increase of the transepidermal water loss TEWL after UV radiation indicating an altered barrier against water loss and thus a deterioration in the water homeostasis and water holding capacities [25–29].

### 3.3 | SSLs play a protective role against solar radiations impact on water kinetics in SC

In order to study the effect of SSLs on SC hydration/dehydration process with and without irradiation, two experimental set-ups were explored as described in the material and methods part:

TABLE 3 Water desorption and global water loss percentages.

	Ctrl-SC	Irr-SC	Ctrl SC + SSLs	Irr-SC + SSLs	SC-Irr-SSLs
Water desorption (WD%)	26%	36%	26%	26%	29%
Global water loss (GWL%)	30%	42%	31%	28%	27%

1. SSLs directly applied on the surface of the SC and equilibrated at 100% RH without irradiation (Ctrl SC + SSLs) and with irradiation (Irr-SC + SSLs).
2. SSLs applied on a CaF<sub>2</sub> slide. SC was equilibrated at 100% RH and then irradiated through the SSLs film (SC-Irr-SSLs).

For Ctrl SC + SSLs and Irr-SC + SSLs, a first concern was the water uptake. As the SSLs forms a continuous lipid layer at the surface of the SC and, contrary to *in vivo*, the water uptake in our experimental set-up is from the 100% RH atmosphere.

WC values for both SSLs coated and uncoated controls, Ctrl SC + SSLs and Ctrl-SC, respectively showed no significant difference (Figure 3A) despite of a tendency of decrease with Ctrl SC + SSLs.

After irradiation, WC of SC-Irr-SSLs showed a 27% decrease compared to control and WC of Irr- SC-SSLs decreased around 23% (Figure 3A). The decrease values are significantly lower ( $p$ -value <0.05) compared to irradiated non-protected SC (Irr-SC). Adding SSLs seems to have a role in the protection of the WC properties of the SC.

For WR values, Irr-SC + SSLs showed a 24% decrease while SC-Irr-SSLs presented 32% decrease compared to control (Figure 3B). For LTWH, Irr-SC + SSLs showed a decrease of 20% and SC-Irr-SSLs 24% (Figure 3C). All values are significantly lower than the 53% and 54% observed with Irr-SC ( $p$ -value <0.05) for WR and LTWH, respectively.

The presence of SSLs either directly on the surface of the SC or on a slide (not in contact with the SC) seems to play a protective layer against the alteration of the hydration and drying process of the SC.

WD% showed no significant variations between Ctrl-SC, Ctrl SC + SSLs, and Irr-SC + SSLs with a WD% of 26% while for SC-Irr-SSLs the WD% was only 29% showing a good preservation of the barrier function in presence of SSLs.

Finally, the GWL% showed slightly lower values in presence of SSLs with 31% for Ctrl SC + SSLs, 28% for Irr-SC + SSLs, and 27% for SC-Irr-SSLs compared to Ctrl-SC with a GWL% of 30%. This confirms the preservation of the SC barrier function against water loss in presence of SSLs.

All observations for WC, WR, LTWH, WD%, and GWL% confirm that the presence of SSLs confers a protection of the water uptake mechanism and water loss process of the SC. Given that similar results were obtained from Irr-SC + SSLs (SSLs in contact with the SC) and SC-Irr-SSLs (SSLs applied on a separate slide); one can conclude that, (i) the protective role of SSLs against solar radiations is more likely to be as an optical filter by absorbing a part of the energy of the solar light; (ii) irradiation through SSLs applied on transparent slides can be used to avoid direct application on SC.

### 3.4 | Solar radiations modify SSLs composition

To confirm the solar light absorption by the SSLs and to understand how they participate to the protection of the skin against solar radiations impact, SSLs were submitted to different doses and lipids composition was analyzed using HT-GC/MS.

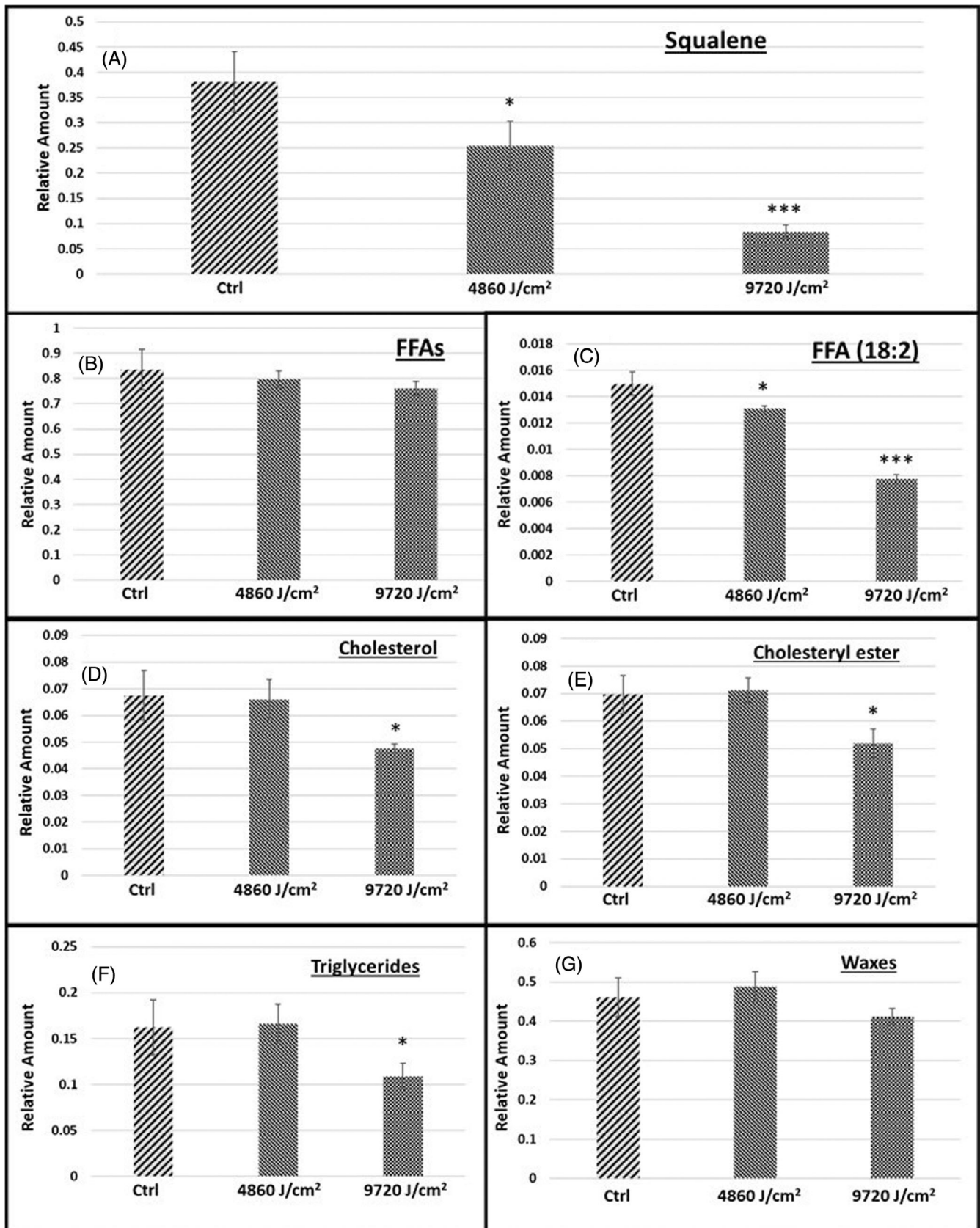
Covering the surface of the SC, the hydrolipidic film is first-line targets of solar radiations [50]. In addition of Vitamin E, that was identified as the first and the predominant anti-oxidant, squalene (Sq), cholesterol (Chol), and fatty acids (FFA) are also known as targets of solar radiations in the SSLs complex [50].

Squalene is the most abundant oxidizable component of SSLs. It is suggested to be the initial target of skin lipid oxidation. It is a linear polyunsaturated triterpene that contains six double bonds [51–53].

The integrated peak areas of squalene, cholesterol, cholesterol esters, fatty acids, FA 18:2, waxes, and triglycerides obtained from HTGC/MS are presented in Figure 4.

A marked decrease of squalene after 3 h of irradiation (4860 J/cm<sup>2</sup>) and a significant decrease ( $p$ -value = 0.008) after 6 h of irradiation (9720 J/cm<sup>2</sup>) were observed (Figure 4A). These results are in concordance with results found in previous studies, the degradation of squalene after irradiation [46, 50, 54].

Regarding fatty acids, the polyunsaturated fatty acids (PUFAs) that contain two or more double bonds, are more prone to lipid oxidation. No significant variation was observed after 3 or 6 h of irradiation on the whole



\* p-value < 10%, \*\* p-value < 5%, \*\*\* p-value < 1 %

FIGURE 4 Impact of solar radiations on SSLs lipid classes.

class of fatty acids (Figure 4B). However, the linoleic acid which contains two double bonds (C18:2) showed the same variation as squalene. Marked and significant decreases were observed after 3 and 6 h of irradiation, respectively (Figure 4C).

Cholesterol has shown the same tendency as squalene and PUFA with a lower variation after 3 and 6 h (Figure 4D).

These results are in concordance with previous studies that showed that squalene is markedly degraded as compared to cholesterol, triglycerides, or FFAs after solar irradiation of SSLs [55, 56].

For esterified lipid classes (triglycerides, waxes, and cholesteryl ester), no significant variations were observed after 3 and 6 h of irradiation. This can be due to the stability of the ester function (Figure 4).

Thus, squalene and PUFAs are the most important ones that play an antioxidant role and protect the skin. Thus, SSLs play a protective role for the skin barrier through the synergy of two aspects, the antioxidant aspect of squalene and PUFAs which constitute 10%–20% of SSLs and the stability aspect against solar radiations by the majority of classes.

## 4 | CONCLUSION

In this work, we developed on novel approach to evaluate the effect of regular solar radiations on SC and the protective action of applied molecules. It is based on SC hydration and dehydration kinetics using of Raman spectroscopy. Different markers were suggested to characterize the water homeostasis, that is, the *WC* which is the capacity of SC to capture water from a highly hydrated atmosphere; the *WR* which represents the remaining water after 1.5 h of the beginning of the drying process; the *WD%* which is an indicator of the water loss rate; and finally, the *LTWH* capacity and the *GWL%* which represent the *LTWH* capacities of the SC.

The first part of the study showed that solar radiations alter all hydration cycle parameters indicating an alteration of *WC* sites as well the *WR* and holding capacities.

In addition to that, this work shows that the presence of SSLs confers a protection of the water uptake mechanism and water loss process of the SC.

Either directly applied on the surface of the SC or put on a slide (not in contact with the SC), the SSLs seem to play the same protective role against the alteration of the hydration and drying process of the SC. Thus, the protective role of SSLs against solar radiations is more as an optical filter by absorbing a part of the energy of the solar light. In addition, and to confirm the solar light

absorption by the SSLs, a significant decrease was observed of squalene and PUFAs after irradiating the SSLs and analyzing it in HT-GC/MS. However, cholesterol the same tendency as squalene and PUFA with a lower variation and for the esterified lipid classes (triglycerides, waxes, and cholesteryl ester), no significant variations were observed due to the stability of their ester function.

Finally, SSLs play an important protective role for the skin barrier through the synergy of two aspects, the antioxidant aspect of squalene and PUFAs which constitute 10%–20% of SSLs and the stability aspect against solar irradiation by most other classes.

In the second part of this study, the protective effect of sunscreen formulations in the preservation of water homeostasis in the SC and their possible synergic action with SSLs will be explored.

## ACKNOWLEDGMENTS

The authors would like to thank the Center of Research Pierre Fabre Dermo Cosmetics for the financial support of this work.

## CONFLICT OF INTEREST STATEMENT

The authors declare that they have no conflict of interest.

## DATA AVAILABILITY STATEMENT

The data that support the findings of this study are available from the corresponding author upon reasonable request.

## ORCID

Ali Assi  <https://orcid.org/0000-0002-5019-0100>

Ali Tfayli  <https://orcid.org/0000-0002-9222-2852>

## REFERENCES

- [1] A. Nicolaou, S. M. Pilkington, L. E. Rhodes, *Chem. Phys. Lipids* **2011**, *164*, 535.
- [2] V. T. Natarajan, P. Ganju, A. Ramkumar, R. Grover, R. S. Gokhale, *Nat. Chem. Biol.* **2014**, *10*, 542.
- [3] B. Breiden, H. Gallala, T. Doering, K. Sandhoff, *Eur. J. Cell Biol.* **2007**, *86*, 657.
- [4] C. W. Franzke, C. Cobzaru, A. Triantafyllopoulou, S. Loffek, K. Horiuchi, D. W. Threadgill, T. Kurz, N. van Rooijen, L. Bruckner-Tuderman, C. P. Blobel, *J. Exp. Med.* **2012**, *209*, 1105.
- [5] V. van Drongelen, M. Alloul-Ramdhani, M. O. Danso, A. Mieremet, A. Mulder, J. van Smeden, J. A. Bouwstra, A. el Ghalbzouri, *Exp. Dermatol.* **2013**, *22*, 807.
- [6] F. F. Sahle, T. Gebre-Mariam, B. Dobner, J. Wohlrab, R. H. Neubert, *Skin Pharmacol. Physiol.* **2015**, *28*, 42.
- [7] J. van Smeden, J. A. Bouwstra, *Curr. Probl. Dermatol.* **2016**, *49*, 8.
- [8] V. Mlitz, J. Latreille, S. Gardinier, R. Jdid, Y. Drouault, P. Hufnagl, L. Eckhart, C. Guinot, E. Tschachler, *J. Eur. Acad. Dermatol. Venerol.* **2012**, *26*, 983.

- [9] R. Vyumvuhore, A. Tfayli, H. Duplan, A. Delalleau, M. Manfait, A. Baillet-Guffroy, *Analyst* **2013**, *138*, 4103.
- [10] E. Sylvie. *PhD Thesis*, Ecole polytechnique de l'Université de Nantes (France) **2003**.
- [11] L. D. Rhein, F. A. Simion, C. Froebe, J. Mattai, R. H. Cagan, *Colloids Surf* **1990**, *48*, 1.
- [12] J. W. Fluhr, R. Darlenski, C. Surber, *Br. J. Dermatol.* **2008**, *159*, 23.
- [13] P. G. Sator, J. B. Schmidt, H. Honigsmann, *J. Am. Acad. Dermatol.* **2003**, *48*, 352.
- [14] C. Berkey, N. Oguchi, K. Miyazawa, R. Dauskardt, *Biochem. Biophys. Rep.* **2019**, *19*, 100657.
- [15] R. Lucas, T. McMichael, W. Smith, B. K. Armstrong, A. Prüss-Üstün, World Health Organization, *Solar Ultraviolet Radiation: Global Burden Of Disease From Solar Ultraviolet Radiation/Robyn Lucas ... [et al.]; Editors, Annette Prüss-Üstün ... [et al.]*, World Health Organization, Geneva **2006**.
- [16] A. Assi, S. Tfayli, A. Quatela, F. Bonnier, A. Baillet-Guffroy, A. Tfayli, *Eur. J. Dermatol.* **2022**, *32*, 33.
- [17] M. E. Darvin, I. Gersonde, H. Albrecht, W. Sterry, J. Lademann, *Laser Phys.* **2006**, *16*, 833.
- [18] E. R. Gonzaga, *Am. J. Clin. Dermatol.* **2009**, *10*, 19.
- [19] A. Villaret, C. Ipinazar, T. Satar, E. Gravier, C. Mias, E. Questel, A. M. Schmitt, V. Samouillan, F. Nadal, G. Josse, *Skin Res. Technol.* **2019**, *25*, 270.
- [20] K. Scharffetter-Kochanek, P. Brenneisen, J. Wenk, G. Herrmann, W. Ma, L. Kuhr, C. Meewes, M. Wlaschek, *Exp. Gerontol.* **2000**, *35*, 307.
- [21] J. Lademann, S. Schanzer, M. Meinke, W. Sterry, M. E. Darvin, *Skin Pharmacol. Physiol.* **2011**, *24*, 238.
- [22] M. G. Tosato, D. E. Orallo, S. M. Ali, M. S. Churio, A. A. Martin, L. Dicio, *J. Photochem. Photobiol., B* **2015**, *153*, 51.
- [23] M. Egawa, H. Iwaki, *Skin Res. Technol* **2008**, *14*, 410.
- [24] T. Gambichler, B. Künzlberger, V. Paech, A. Kreuter, S. Boms, A. Bader, G. Moussa, M. Sand, P. Altmeyer, K. Hoffmann, *Clin. Exp. Dermatol.* **2005**, *30*, 79.
- [25] S. Meguro, Y. Arai, K. Masukawa, K. Uie, I. Tokimitsu, *Photochem. Photobiol.* **1999**, *69*, 317.
- [26] C. Gélis, A. Mavon, M. Delverdiere, N. Paillous, P. Vicendo, *Photochem. Photobiol.* **2002**, *75*, 598.
- [27] Y. Takagi, H. Nakagawa, H. Kondo, Y. Takema, G. Imokawa, *J Invest. Dermatol.* **2004**, *123*, 1102.
- [28] S. H. Yoon, J. I. Park, J. E. Lee, C. H. Myung, J. S. Hwang, *Skin Pharmacol. Physiol.* **2019**, *32*, 254.
- [29] S. Mac-Mary, J.-M. Sainthillier, A. Jeudy, C. Sladen, C. Williams, M. Bell, P. Humbert, *Clin. Interv. Aging* **2010**, *5*, 277.
- [30] K. Biniek, K. Levi, R. H. Dauskardt, *Proc. Natl. Acad. Sci. USA.* **2012**, *16*, 17111.
- [31] R. Vyumvuhore, A. Tfayli, M. Manfait, A. Baillet-Guffroy, A. Baillet-Guffroy, *Skin Res. Technol.* **2014**, *20*, 282.
- [32] K. Biniek, A. Tfayli, R. Vyumvuhore, A. Quatela, M. F. Galliano, A. Delalleau, A. Baillet-Guffroy, R. H. Dauskardt, H. Duplan, *Exp. Dermatol.* **2018**, *27*, 901.
- [33] M.-F. Galliano, A. Tfayli, R. H. Dauskardt, B. Payre, C. Carrasco, S. Bessou-Touya, A. Baillet-Guffroy, H. Duplan, *Exp. Dermatol.* **2021**, *30*, 1352.
- [34] A. Mavon, H. Zahouani, D. Redoules, P. Agache, Y. Gall, P. Humbert, *Colloids Surf., B* **1997**, *8*, 147.
- [35] J. J. Thiele, S. U. Weber, L. Packer, *J. Invest. Dermatol.* **1999**, *113*, 1006.
- [36] G. S. K. Pilgram, J. van der Meulen, G. S. Gooris, H. K. Koerten, J. A. Bouwstra, *Biochim. Biophys. Acta* **2001**, *1511*, 244.
- [37] M. Q. Man, S. J. Xin, S. P. Song, S. Y. Cho, X. J. Zhang, C. X. Tu, K. R. Feingold, P. M. Elias, *Skin Pharmacol. Phys.* **2009**, *22*, 190.
- [38] R. S. Greene, D. T. Downing, P. E. Pochi, J. S. Strauss, *J. Invest. Dermatol.* **1970**, *54*, 240.
- [39] D. T. Downing, P. W. Wertz, M. E. Stewart, *Int. J. Cosmet. Sci.* **1986**, *8*, 115.
- [40] D. Saint-LÉGÉR, J. L. LÉVÉQUE, *Int. J. Cosmet. Sci.* **1980**, *2*, 283.
- [41] M. Vantrou, P. Y. Venencie, J. C. Chaumeil, *Ann. Dermatol. Venereol.* **1987**, *114*, 1115.
- [42] G. Pablo, A. Hammons, S. Bradley, J. E. Fulton Jr., *J. Invest. Dermatol.* **1974**, *63*, 231.
- [43] A. R. Shalita, *J. Invest. Dermatol.* **1974**, *62*, 332.
- [44] N. Nicolaidis, *Science* **1974**, *186*, 19.
- [45] K. R. Smith, D. M. Thiboutot, *J. Lipid Res.* **2008**, *49*, 271.
- [46] M. Picardo, M. Ottaviani, E. Camera, A. Mastrofrancesco, *Dermatoendocrinol.* **2009**, *1*, 68.
- [47] R. Michael-Jubeli, J. Bleton, A. Baillet-Guffroy, *J. Lipid Res.* **2011**, *52*, 143.
- [48] A. Rigal, R. Michael-Jubeli, A. Bigouret, A. Nkengne, D. Bertrand, A. Baillet-Guffroy, A. Tfayli, *Eur. J. Dermatol.* **2020**, *30*, 103.
- [49] A. Tfayli, D. Jamal, R. Vyumvuhore, M. Manfait, A. Baillet-Guffroy, *Analyst* **2013**, *138*, 6582.
- [50] S. Ekanayake Mudiyanse, M. Hamburger, P. Elsner, J. J. Thiele, *J. Invest. Dermatol.* **2003**, *120*, 915.
- [51] N. Shimizu, J. Ito, S. Kato, Y. Otoki, M. Goto, T. Eitsuka, T. Miyazawa, K. Nakagawa, *Sci. Rep.* **2018**, *8*, 9116.
- [52] V. Kostyuk, A. Potapovich, A. Stancato, C. De Luca, D. Lulli, S. Pastore, L. Korkina, *PLoS One* **2012**, *7*, e44472.
- [53] E. Niki, *Free Radical Res.* **2015**, *49*, 827.
- [54] K. J. Dennis, T. Shibamoto, *Photochem. Photobiol.* **1989**, *49*, 711.
- [55] C. De Luca, G. Valacchi, *Mediators Inflamm.* **2010**, *2010*, 321494.
- [56] M. Picardo, C. Zompetta, C. De Luca, M. Cirone, A. Faggioni, M. Nazzaro-Porro, S. Passi, G. Prota, *Arch. Dermatol. Res.* **1991**, *283*, 191.

**How to cite this article:** A. Assi, R. Michael-Jubeli, H. Duplan, A. Baillet-Guffroy, C. Jacques-Jamin, A. Tfayli, *J. Biophotonics* **2023**, *16*(8), e202300055. <https://doi.org/10.1002/jbio.202300055>